HHS Public Access

Author manuscript

Arch Biochem Biophys. Author manuscript; available in PMC 2017 July 01.

Published in final edited form as:

Arch Biochem Biophys. 2016 July 1; 601: 80–87. doi:10.1016/j.abb.2016.03.010.

Role of Cardiac Troponin I Carboxy Terminal Mobile Domain and Linker Sequence in Regulating Cardiac Contraction

Nancy L. Meyer[*] and **P. Bryant Chase**[†]

[*]Department of Biochemistry and Molecular Biology, Oregon Health and Science University, Portland, Oregon, USA

[†]Department of Biological Science and Program in Molecular Biophysics, Florida State University, Tallahassee, Florida, USA

Abstract

Inhibition of striated muscle contraction at resting Ca^{2+} depends on the C-terminal half of troponin I (TnI) in thin filaments. Much focus has been on a short inhibitory peptide (Ip) sequence within TnI, but structural studies and identification of disease-associated mutations broadened emphasis to include a larger mobile domain (Md) sequence at the C-terminus of TnI. For Md to function effectively in muscle relaxation, tight mechanical coupling to troponin's core—and thus tropomyosin—is presumably needed. We generated recombinant, human cardiac troponins containing one of two TnI constructs: either an 8-amino acid linker between Md and the rest of troponin ($cTnI_{Link8}$), or an Md deletion ($cTnI_{1\text{-}163}$). Motility assays revealed that Ca^{2+}-sensitivity of reconstituted thin filament sliding was markedly increased with $cTnI_{Link8}$ (~0.9 pCa unit leftward shift of speed-pCa relation compared to WT), and increased further when Md was missing entirely (~1.4 pCa unit shift). Cardiac Tn's ability to turn off filament sliding at diastolic Ca^{2+} was mostly (61%), but not completely eliminated with $cTnI_{1\text{-}163}$. TnI's Md is required for full inhibition of unloaded filament sliding, although other portions of troponin—presumably including Ip—are also necessary. We also confirm that TnI's Md is not responsible for superactivation of actomyosin cycling by troponin.

GRAPHICAL ABSTRACT

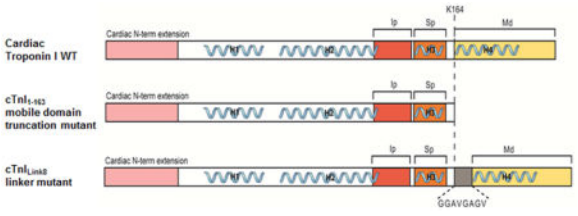

Address correspondence to: P. Bryant Chase, Ph.D., F.A.H.A., Department of Biological Science, Florida State University, Biology Unit One, 81 Chieftain Way, Box 3064370, Tallahassee, FL 32306-4370, USA, chase@bio.fsu.edu, Voice: 850-644-0392, Fax: 850-644-0481.

Keywords

Heart; thin filament; in vitro motility assay; unloaded filament sliding; calcium; excitation-contraction coupling

INTRODUCTION

Troponin is an essential component in the Ca^{2+}-mediated regulation and modulation of striated muscle contraction [1,2]. Detailed knowledge about the structure and function of troponin is essential not only for understanding excitation-contraction coupling in striated muscle, but also for insight into familial cardiomyopathies [3–5] and skeletal myopathies [6–8] that are associated with mutations in troponin.

Of troponin's three polypeptide subunits, troponin I (TnI) deserves particular attention because it is central—both structurally and functionally—to thin filament control and modulation of striated muscle contraction. TnI's designation derives from its ability to inhibit actomyosin interactions on its own (without troponin C, troponin T or tropomyosin) by binding F-actin, regardless of whether Ca^{2+} is present [9]. A highly conserved and centrally located peptide of TnI was identified with much of TnI's inhibitory activity [10,11] although in the context of the ternary troponin complex, however, it is clear that other portions of TnI in addition to this inhibitory peptide (Ip) are required for full inhibition of actomyosin activity in the absence of Ca^{2+} [12–14]. Structurally, TnI is central to the troponin complex through: (i) formation of a stable α-helical coiled-coil with troponin T (TnT, which interacts with tropomyosin); (ii) separate interactions with the C-terminal and N-terminal domains of troponin C (TnC, which binds divalent cations including regulatory Ca^{2+}); and (iii) multiple interacting segments, including Ip, with F-actin [15–21]. Ca^{2+} binding to the N-domain of TnC shifts the bias for portions of TnI from interacting with F-actin under relaxing (diastolic) conditions, to interacting with TnC and unbinding from F-actin under activating (systolic) conditions. These Ca^{2+}-dependent changes in TnI-TnC interactions modulate regulatory unit structure, and determine whether strong cross-bridge formation and contraction can occur.

TnI's primary actin-binding regions are located in the C-terminal half of both the skeletal (sTnI) and the longer cardiac (cTnI) isoform. The Ip is immediately C-terminal to an α-helix (H2) that forms a coiled-coil with TnT (IT-arm). Following TnI's primary sequence from Ip toward the C-terminus are the switch domain (or switch peptide, Sp) and the much larger mobile domain (Md). These segments of TnI are separated by short, connecting sequences. Md was identified as mobile relative to the rest of the ternary troponin complex due to its "visibility" by NMR spectroscopy [22]; this observation suggests that Md is connected to the rest of the troponin complex by a flexible linker sequence. Murakami et al. [22] determined a solution structure for Md and also showed that isolated Md binds F-actin. Crystal structures of troponin, however, do not resolve Md [16,17], and solution studies by Sykes and colleagues indicate that most Md molecules are typically disordered when not bound to F-actin [23,24] which further reinforces the idea that Md truly is mobile, at least in some physiologically relevant circumstances such as the presence of activating Ca^{2+}

(systole). While there is general agreement that the C-terminus of TnI is crucial for thin filament regulation, and that the structure of the C-terminus varies with Ca^{2+} and other thin filament proteins [20–28], several questions remain about the relative importance of Md versus other parts of TnI's C-terminus and the significance of a putative flexible linker connecting Md to the rest of TnI, the troponin complex, and the rest of the regulatory unit including tropomyosin.

The overall goal of this study was to determine the relative importance of cTnI's Md for Ca^{2+}-regulation of cardiac thin filament sliding. We hypothesized that the flexible linker sequence between TnI's switch peptide and Md, and specifically the length of the linker sequence, is critical for Md's role in Ca^{2+}-regulation of the cardiac thin filament. We report on two constructs of human cardiac TnI (Fig. 1A) assayed within the troponin complex: one construct has an extended, flexible linker connecting Md to the rest of cTnI ($cTnI_{Link8}$) that allows us to test our hypothesis, and the second construct allows us to determine what happens when Md is missing entirely ($cTnI_{1\text{-}163}$). Using motility assays with reconstituted thin filaments, we found that it is markedly easier for Ca^{2+} to activate filament sliding (leftward shift of Ca^{2+}-sensitivity) when cTn contains $cTnI_{Link8}$, and even more so when Md is removed. In addition, the ability of cTn to turn off filament sliding at low (diastolic) Ca^{2+} levels was mostly, but not completely eliminated for the $cTnI_{1\text{-}163}$ construct. These observations have implications for structure-function relation between Md, the rest of the cardiac troponin complex, and thin filament regulation by Ca^{2+}.

MATERIALS and METHODS

Rabbit skeletal muscle protein preparations

Relevant protein purification procedures have been described previously [29–40]. Skeletal muscle myosin and actin were isolated from the muscle of adult New Zealand White rabbits. Rabbit procedures were approved by Florida State University's Animal Care and Use Committee and rabbits were handled in accordance with the current National Institutes of Health/National Research Council Guide for the Care and Use of Laboratory Animals. Heavy meromyosin (HMM) was prepared according to Kron et al. [41] and stored at 4°C for up to three days [29–33]. ATP-insensitive heads were removed by ultracentrifugation [41] and competent HMM diluted to the final working concentration (typically 250 μg/ml). Filamentous actin (F-actin) was purified from fast skeletal muscle acetone powder and stored at 4°C for up to one month [29–33,41,42]. Actin concentration was determined spectroscopically in globular (G-actin) form prior to labeling and purity was assessed by gel electrophoresis. F-actin was labeled with rhodamine-phalloidin (RhPh) (Invitrogen) and RhPh F-actin was diluted to 8 nM in actin buffer (AB) without added ATP (25 mM KCl, 25 mM imidazole, 4 mM $MgCl_2$, 1 mM EGTA, 1 mM dithiothreitol (DTT), pH 7.4) [41].

Coexpression and purification of recombinant human cardiac troponin complexes containing WT or mutant troponin I

Human cardiac troponin complex (rhcTn) was recombinantly expressed in *E. coli* and purified as previously reported [29–32,43]. Briefly, cTnT, cTnI, and cTnC were coexpressed from a pET41a plasmid (Novagen-EMD Biosciences, San Diego, CA, USA) (Fig. 2) with a

glutathione S-transferase (GST) tag incorporated at the N-terminus of cTnT, a site distal from the cTnI/cTnC binding region at cTnT's C-terminus. Affinity column purification of fusion GST-rhcTn followed by GST tag cleavage with TEV protease leaves an N-terminal extension of rhcTnT of a single amino acid (Gly). SDS-PAGE gels indicate a resulting complex that is highly pure and functional as corroborated by motility assay controls (see below). Concentrations were determined as reported [29–32,43,44] and aliquots stored at −80°C.

Mutant rhcTn complexes were engineered by site-directed PCR mutagenesis (PCR-SDM) of the WT cTnI gene which was cloned into a pCR 2.1 TOPO vector (Invitrogen) to generate two cTnI constructs (Fig. 1): a shorter cTnI missing Md ($cTnI_{1\text{-}163}$), and a longer cTnI containing an 8-amino acid, flexible linker inserted immediately N-terminal to Md ($cTnI_{Link8}$). Mutant $cTnI_{Link8}$ contains eight residues of flexible linker sequence (Gly-Gly-Ala-Val-Gly-Ala-Gly-Val) inserted C terminal to WT residue K164 via the corresponding DNA sequence: 5′ GGT GGT GCA GTT GGN GCA GGT GTT 3′. Linker length of eight amino acids was chosen as the longest polypeptide sequence (maximum extension ~ 3 nm) that could be introduced that was less than the distance between actin monomers in the thin filament, i.e., a distance comparable to or longer than the azimuthal distance traversed by Tm when a regulatory unit switches on or off, but less than the axial periodicity of Md binding sites along the thin filament [20–22]. To generate the truncated mutant without Md, $cTnI_{1\text{-}163}$, three adjacent UAA (bacterial STOP) codons were inserted immediately prior to K164 codon [32]. Mutated cTnI gene constructs were cloned back into the pET41a coexpression vector (Fig. 2) and expressed and purified as described for WT rhcTn. Differences in pI for purified proteins were estimated to be less than 0.1 unit for both mutants. No change to the extinction coefficient used to quantify the $cTnI_{Link8}$ complex was deemed necessary; for the smaller $cTnI_{1\text{-}163}$ complex, we used an extinction coefficient at A_{280} of 24420 M^{-1} cm^{-1} calculated with Scripps Protein Calculator v3.3 [44].

Expression and purification of recombinant human α-tropomyosin

Human striated muscle-specific α-tropomyosin (Tm) was recombinantly expressed in *E. coli* as previously described [31–33,43]. Concentrations were determined spectroscopically and aliquots stored at −80°C. Purified homodimeric GS-α-tropomyosin contained two extra N-terminal amino acids (Gly-Ser), which represents a conservative alternative [31–33,43] to the AS-dipeptide in other bacterially expressed tropomyosins that substitutes functionally for N-terminal acetylation [45,46].

In vitro motility assays

In vitro motility assays with regulated thin filaments were carried out using methods described previously [29–40,47–50]. Flow cells with nitrocellulose-coated substrates were prepared as reported [29–40,47–50] and room-temperature solutions were left for 1 min in the chamber, each followed by flushes of AB, in the following order: HMM, blocking solution (0.5 mg ml^{-1} bovine serum albumin (BSA) in AB), unlabeled, sheared F-actin, 0.5 mM ATP buffer (to passivate HMM that binds actin in an ATP-insensitive manner), RhPh-labeled F-actin, and wash buffer (WB) (AB plus rhcTn and Tm) [39,41,51]. WB was incubated in the chamber for 3 min, allowing assembly of regulatory complexes onto F-actin

to form regulated thin filaments. Motility was initiated by motility buffer (MB) (2 mM MgATP, 1 mM Mg^{2+}, 10 mM EGTA, calcium acetate to achieve the desired pCa between 9 and 4 (pCa = − log [Ca^{2+}], where [Ca^{2+}] is in molar), 50 mM K^+, 15 mM Na^+, 20 mM MOPS, 0.085 M Γ/2 adjusted with $Tris^+$ as the cation and acetate as the anion, pH 7.0 at 30°C, and 0.3% methylcellulose (MC). Tm and rhcTn construct were added at the appropriate concentration (see Results and discussion). MB also contained 3 mg/ml glucose, 100 μg/ml glucose oxidase, 18 μg/ml catalase, and 40 mM DTT to minimize photobleaching during imaging and recording of motility assays.

Microscopy and acquisition

Flow cells were imaged on a Nikon Eclipse TE2000-U inverted fluorescence microscope (Nikon Corporation, Tokyo, Japan) with both Hg and TIRF illumination. Temperature within flow cells was maintained at ~ 30°C by an objective heater coil (20/20 Technology, Inc., Wilmington, NC, USA). RhPh-labeled filaments were imaged with a SIT camera (Model VE1000; Dage-MTI, Michigan City, IN) and video recorded onto DVD at 30 frames s^{-1}. Typically, six fields were recorded for > 30 s each for every flow cell. Total imaging time per flow cell was 5–10 min (Fig. 3).

Data analysis

Filament sliding speeds were quantified with ImageJ (v1.41; W.S. Rasband, NIH, Bethesda, MD, USA). Data from each field were converted into stacks of 90 frames using VirtualDub 1.8.6 (Copyright © 1998–2008 Avery Lee), yielding a sampling of every tenth frame. Stacks were imported into ImageJ and image contrast was enhanced by background subtraction [52]. At least 10–20 filaments were randomly selected per field and the length of the path traveled by a filament determined by manual tracking of its leading edge. This was performed with ImageJ plugin MTrackJ for the duration of a filament's movement or presence within frame boundaries. Average speed (μm s^{-1}) was obtained by dividing distance traveled by the duration of tracking (Fig. 3). The ratio of standard deviation/mean speed was calculated for each path as an indicator of motion uniformity [35,39,53,54]. A filament was accepted as moving uniformly and included in calculation of the unweighted mean speed S in units of μm s^{-1} (± SD) for the field when this ratio was < 0.3. Replicate flow cell data were combined for analyses. A modified form of Sir A. V. Hill's equation for cooperative binding [55] was fit to all raw speed-pCa data using nonlinear least squares regression analysis (SigmaPlot ver 11, Systat Software, Inc., Chicago, IL, USA; and R ver 3.2.3, The R Foundation for Statistical Computing):

$$S = S_{max}\left(1 + 10^{n_H(pCa - pCa_{50})}\right)^{-1} + S_{min} \quad (1)$$

Regression parameter S_{min} represents the speed obtained at low [Ca^{2+}], and S_{max} is the Ca^{2+}-activatable increment in speed. Speed at saturating Ca^{2+} equals $S_{max} + S_{min}$. pCa_{50} is equal to the pCa at the midpoint of the Ca^{2+}-dependent portion of the speed-pCa relationship (i.e., for $S = (S_{max}/2) + S_{min}$) and n_H describes the cooperativity as reflected in the steepness of the relationship plot around pCa_{50}. Data were then normalized to ($S_{max} + S_{min}$).

When S_{min} was not statistically different from 0, the normalized mean speed data (s) were fit to a two-parameter version of the Hill Eq:

$$s=(1+10^{n_H(pCa-pCa_{50})})^{-1} \quad (2)$$

Alternatively, when S_{min} was statistically different from 0 (i.e., significant filament sliding occurred at Ca^{2+} levels that would normally be associated with relaxation), the normalized mean speed data (s) were fit to a three-parameter version of the Hill Eq where the sum, s_{min} + s_{max}, was constrained to be 1.0, and thus $s_{max} = 1 - s_{min}$ (note that s_{max} corresponds to the Ca^{2+}-activatable component of regulated filament sliding):

$$s=(1-s_{min})(1+10^{n_H(pCa-pCa_{50})})^{-1}+s_{min} \quad (3)$$

Errors for regression parameters are SE from the regression.

RESULTS and DISCUSSION

Working concentrations of tropomyosin and troponin constructs for motility assays

Optimal working concentrations of rhcTn and Tm (equal molar ratios of rhcTn and Tm) for motility assays were identified as previously described [29–33,35,39]. For each protein and each set of assays, we determined the minimal concentration required to maximally inhibit motility at pCa 9 (noting that not all of the constructs used in these experiments were capable of turning off motility at pCa 9 regardless the concentration of cTn and Tm), while simultaneously offering maximum speed at pCa 5; in other words, increasing the concentrations (up to 125 nM) of the rhcTn construct (and Tm) did not significantly decrease speed at pCa 9 or increase speed at pCa 5. In the experiments reported here, rhcTn WT was assayed at 25 nM, and the $cTnI_{Link8}$ and $cTnI_{1\text{-}163}$ mutant complexes were assayed at 50 nM. The regulatory protein concentrations that we used in these experiments are similar to typical working concentrations used previously for WT or single amino acid mutants of regulatory proteins that yielded well-regulated thin filaments (15–75 nM) [30,32,33]. Little or no effect on affinity for thin filaments in the presence of Ca^{2+} was anticipated because our modified constructs did not alter the α-helical coiled-coil of the IT-arm, or the N-terminal α-helix of cTnT which binds Tm.

Motility speed-pCa relationship with the wild-type cardiac troponin complex

Maximum sliding velocity (S_{max} + S_{min}, Eq 1) was 10.9 ± 0.7 μm s^{-1} for thin filaments reconstituted with Tm plus rhcTn containing cTnI WT, as compared to 9.2 ± 1.0 μm s^{-1} for unregulated F-actin in experiments with the same HMM preparations, indicating a 1.2-fold increase in the maximum speed when rhcTn WT and Tm (25 nM) are present with saturating Ca^{2+} (unregulated F-actin data not shown). Minimum sliding velocity (s_{min}) achieved at pCa 9 was effectively zero (Figs. 3, 4); the majority of filaments showed no discernable translocation at pCa 9 or exhibited erratic motility (per Material and methods).

Regression on the normalized speed-pCa data (Fig. 4) using Eq 2 yielded parameter estimates (Table 1) for pCa_{50} (~ 6.0) and Hill coefficient n_H (6.6) that are typical of regulated filaments containing rhcTn and α-tropomyosin [29,33,56], and indicate significant, apparent cooperativity for normal Ca^{2+}-activation of filament sliding.

$cTnI_{Link8}$ complex increased Ca^{2+}-sensitivity of filament sliding: loosening the coupling between TnI's mobile domain and troponin's core domain tips the Ca^{2+}-regulatory balance toward "on"

The major effect of incorporating an 8-residue linker into cTnI between Sp and Md was a substantial increase in Ca^{2+}-sensitivity (Fig. 4), with a leftward pCa_{50} shift of almost a full pCa unit compared with WT (0.91 pCa units; Table 1). Filaments containing the $cTnI_{Link8}$ mutant activated fully at pCa 5 (S_{max} = 14.6 ± 1.5 μm s^{-1}) and exhibited no significant, directed movement at pCa 9 (S_{min} = 0.4 ± 1.01 μm s^{-1}); we attribute differences in S_{max} compared with cTnI WT to different batches of HMM (as assayed with unregulated F-actin) and not to an intrinsic property of $cTnI_{Link8}$. Thus, as with cTnI WT data, Eq 2 was used to fit the normalized data for filaments reconstituted with Tm plus rhcTn containing the $cTnI_{Link8}$ mutant (Fig. 4 and Table 1). While Ca^{2+} sensitivity of filament sliding speed was markedly increased, the apparent cooperativity was reduced as indicated by a lower n_H parameter estimate for the $cTnI_{Link8}$ mutant compared with cTnI WT (Table 1).

The introduction of a short (8 amino acid), flexible linker into cTnI was expected to at least partially decouple Md function from that of Sp and Ip. A simple model of the regulatory unit considers interactions among domains within the C-terminus of TnI, TnC and actin: Md and Ip bind actin in relaxing conditions; while Sp binds N-cTnC in the presence of Ca^{2+} [20,21,57]. The consequent tension between these domains is expected to modulate the mobility (and thus position) of Tm on the thin filament. This simple model suggests that partial or complete decoupling—if it occurred—could result in two possible scenarios. In the first scenario with $cTnI_{Link8}$, if Sp binding to N-cTnC in the presence of Ca^{2+} could not pull Md (and Ip) off actin, the engineered flexible linker would reduce the likelihood that regulatory units turn on. In this first case we predicted slower S_{max}, with filaments stopped despite elevated Ca^{2+} in the most extreme case, and/or a rightward shift of the speed-pCa relationship. In the second scenario with $cTnI_{Link8}$, if Md (and Ip) binding to actin in the absence of Ca^{2+} could not pull Sp away from N-cTnC, the additional linker sequence would reduce the likelihood that regulatory units turn off. In this second case we predicted a leftward shift of the speed-pCa relation and/or an elevated S_{min}. While these two possible scenarios are not mutually exclusive, the data in Fig. 4 are clearly compatible with only the second in which the extra, flexible linker is presumed to make it easier for Sp to bind N-cTnC at lower Ca^{2+} levels, and little or no interference with consequent unbinding of Md (and Ip) from actin; this scenario, where the extra linker in $cTnI_{Link8}$ makes it easier for Sp to bind N-cTnC, perhaps by allowing Sp to be closer to N-cTnC in the absence of Ca^{2+} as illustrated schematically in the center of Fig. 5 where the linker is shown as a heavy blue line just N-terminal to Md (for comparison, WT is shown at left in Fig. 5). In the absence of Ca^{2+}, the linker does not enable turning on of regulatory units to permit filament sliding; because very few regulatory units need to be in the on state to allow filament sliding [35,39],

we infer that the entire $cTnI_{Link8}$ thin filament must be off in the absence of Ca^{2+} (Fig. 5, center).

In addition to the possibility of antagonistic pulling between Sp and Md described above, another logical possibility is that these connected domains push one another when troponin either turns a regulatory unit on or off, particularly if they influence the second regulatory unit on the opposite side of the thin filament. Incorporation of an additional eight residues into what is already a flexible linker [22–24] connected to a highly dynamic Md [28,58–60] should disrupt any significant motion that involves Md pushing on the core domain of Tn and thus on Tm, too. While we consider this possibility unlikely, any pushing of Md on other parts of a regulatory unit would have to stabilize the off state to be consistent with our data.

The simple model discussed above deserves to be expanded with a broader view of the entire regulatory unit plus the cross-bridges that interact with that unit. Our measurements report on the functional state of thin filaments, rather than the structure of TnC, the locations of specific domains within TnI, or other specific structural components of thin filament regulatory units [61–63]. It is possible that $cTnI_{Link8}$ allows Tm to move away from the position in which it blocks myosin-binding sites on actin independent of Sp binding to N-cTnC. The absence of motility at low Ca^{2+} (Figs. 3, 4) argues against substantial displacement of Tm simply due to the presence of the linker. Furthermore, the low value of the cooperativity parameter n_H for $cTnI_{Link8}$ argues that the linker does not enhance the cooperative role of cross-bridges in Ca^{2+}-activation of filament sliding.

Clearly the additional linker sequence in the $cTnI_{Link8}$ construct does not completely decouple Md from the rest of troponin, and also does not likely influence any functions of Md that are independent of its physical connection to Sp. For example, studies in which portions of Ip were replaced with flexible peptide sequences (not extended linkers) suggest that the Ip sequence within the Tn complex has a substantial role in Ca^{2+}-regulation of ATPase activity [64], in agreement with prior studies on changes in Ip sequence [11,29,30,65–67]; perhaps the presence of an intact Ip in the $cTnI_{Link8}$ construct largely overcomes the decoupling of Md from the rest of Tn. It is also possible that the novel linker sequence in $cTnI_{Link8}$ itself has unintended effects, perhaps by binding to TnC. In addition to these possibilities, it has been suggested that the extreme C-terminus of cTnI stabilizes the Ca^{2+}-activated structure of regulatory units [27], and this property could be facilitated by the $cTnI_{Link8}$ construct.

We therefore extended our study by examining a cTnI construct ($cTnI_{1\text{-}163}$) [32] that is missing the entire Md, and also does not contain the additional linker sequence that is present in TnI_{Link8}.

$cTnI_{1\text{-}163}$ complex displays increased Ca^{2+}-sensitivity and incomplete inhibition at low Ca^{2+}: TnI's mobile domain is critical for complete regulation in the absence of Ca^{2+}

Filaments regulated with $cTnI_{1\text{-}163}$ displayed maximum sliding speeds comparable to those of the other regulated filaments in this study. Regression analysis of the raw data (Eq 1) gave S_{max} = 14.8 ± 0.6 μm s^{-1} and S_{min} = 9.0 ± 0.4 μm s^{-1}. The minimum sliding speed at pCa 9

was higher than with cTn with cTnI WT or $cTnI_{Link8}$, with the net result that $cTnI_{1-163}$ filaments were unable to achieve full inhibition at low Ca^{2+} (Fig. 4). Normalized sliding speed s_{min} (Eq 3) at low Ca^{2+} was ~ 61% of that achieved at saturating Ca^{2+} ($s_{max} + s_{min}$; Table 1). Also notable in the $cTnI_{1-163}$ assays was a dramatic increase in Ca^{2+} sensitivity of almost 1.5 pCa units relative to WT (Table 1). Note that, while the $cTnI_{Link8}$ data indicated a reduction in the apparent cooperativity for Ca^{2+}-activation of filament sliding when Md is partially decoupled from the regulatory unit, the $cTnI_{1-163}$ data in Fig. 4 did not allow us to determine a reliable value for n_H because of the reduced amplitude for Ca^{2+}-activated speed, s_{max} (Table 1).

Our results indicate that TnI's Md is essential for full inhibition of Ca^{2+}-regulated filament sliding in the in vitro motility assay (Fig. 4), and structural changes that could explain these results are illustrated schematically in Fig. 5 (right). These results (Fig. 4) and the structural model (Fig. 5) are consistent with previous ATPase measurements [12,13], although the changes in Ca^{2+}-sensitivity due to removal of Md were larger in assays of filament sliding (Fig. 4).

Defects in the C-terminus of TnI are found in a number of myopathies, and the functional effects observed using our constructs (Fig. 4) inform the consequences of disease-associated defects. Interestingly, mutations in cTnI that cause inherited forms of hypertrophic or restrictive cardiomyopathies are most prevalent within the C-terminal region and, in qualitative agreement with the observations reported here (Fig. 4), most mutations increase Ca^{2+}-sensitivity and in some cases also exhibit partial loss of regulation at low Ca^{2+} [4,34,68–75]. Mutations in the C-terminal region of sTnI, including truncations, are associated with distal arthrogryposis and also result in increased Ca^{2+}-sensitivity, often with partial loss of regulation at low Ca^{2+} [6–8,76–78]. Furthermore, the C-terminus of cTnI is cleaved in myocardial stunning [79–82]. While the extent of proteolysis ($cTnI_{1-193}$) is not as extreme as removal of the entire Md in our construct described here ($cTnI_{1-163}$), the functional consequences fit with the picture described above for the various mutants and constructs of TnI that affect the C-terminus. Interestingly for $cTnI_{1-193}$ proteolysis in myocardial stunning, the consequences of Md removal (Ca^{2+} sensitization, partial loss of inhibition, and reduced cooperativity) are qualitatively captured by removal of just 3 – 5 residues from the C-terminus of cTnI [56], although not surprisingly the effects are quantitatively larger for $cTnI_{1-163}$ (Fig. 4).

As discussed above, our $cTnI_{Link8}$ data are consistent with Md having a role in stabilizing the off state of regulatory units at low Ca^{2+}, but could also be explained if the extreme C-terminus of Md—alternatively or additionally—stabilized the Ca^{2+}-activated position of tropomyosin, as predicted from thin filament structures obtained with $cTnI_{1-193}$ [27]. Our functional studies with $cTnI_{1-163}$ (Fig. 4), however, indicate that the primary role of Md is stabilizing the off state of regulatory units at low Ca^{2+}. While Md may have a secondary, activating role in some circumstances such as partial Ca^{2+}-activation, we observed that filament sliding was fully activated at saturating Ca^{2+} levels and that Ca^{2+}-sensitivity of filament sliding was greatly enhanced even in the absence of Md (Figs. 4, 5).

The $cTnI_{1-163}$ data in Fig. 4 also demonstrate that other portions of TnI must be involved in turning off thin filament regulatory units at low Ca^{2+} because filament sliding is only partially activated at high pCa when Md is missing. Presumably Ip is the other significant portion with regard to Ca^{2+}-dependent movement between actin and TnC [12,83]. Comparing our study (Fig. 4) with amino acid substitution studies within Ip [11,64], it appears that neither Ip nor Md is sufficient without the other to completely turn off regulatory units at low Ca^{2+} [12–14] and thus they must work together. We have previously suggested that the C-terminus of cTnT (which is located along with cTnI's Md at the C-terminal end of the IT-arm, and was present in all rhcTn complexes used in this study) aids the Ca^{2+}-regulatory function of cTnI's Ip [29], and this could be facilitated by proximity of the extreme C-terminus of cTnT not only to the C-terminus of cTnI, but also to N-cTnC (Fig. 5). We note here however that Md, which is much larger than the C-terminus of cTnT, is predominant for thin filament inhibition.

Our results with $cTnI_{Link8}$ that partially decouples Md function from Sp (and Ip) compelled us to ask what happens when Md (and the engineered linker sequence) is not present. In one sense, the $cTnI_{1-163}$ construct is the most practical yet extreme approach to complete decoupling between Md and Sp. Resorting to insertion of longer linker sequences could permit Md binding to the next actin monomer in the periodic structure of the thin filament's actin core, potentially confounded what should otherwise be the decoupling effects of the linker. We also chose not to add exogenous Md while studying the $cTnI_{1-163}$ construct because that could lead to non-stoichiometric binding along F-actin, i.e., 1:1 Md:actin monomer binding at sufficiently high concentrations which is much higher than the 1:7 binding in the physiologically relevant structure. Even if we limited the binding to ~ 1:7 at low concentrations of exogenous Md, we would still miss out on the physiologically relevant structural relationship with Md binding only to an actin monomer at the same level as Tn's core domain.

Confirmation that cTnI's mobile domain is not responsible for superactivation of filament sliding speed

A number of prior reports have demonstrated that the maximum sliding speed for regulated thin filaments, reconstituted with either cardiac or skeletal muscle regulatory proteins, is markedly faster that sliding speed of F-actin measured using the same preparation of HMM [29–32,34,35,38–40,47,53,84–88]. It has been proposed that this superactivation of filament sliding speed may be related to superactivation of myosin MgATPase (in the absence of actin) due to a direct interaction between troponin and myosin [32].

We confirm here the result of our previous test of the hypothesis that cTnI's Md could be responsible for superactivation of maximum sliding speed: maximum sliding speed (pCa 5) of filaments reconstituted with the $cTnI_{1-163}$ construct was not slower than that for WT as would be expected if Md were responsible for superactivation of filament sliding [32]. Similarly, maximum sliding speed (pCa 5) of filaments reconstituted with the $cTnI_{Link8}$ construct was not distinguishable from that with the $cTnI_{1-163}$ construct. Thus portions of troponin other than Md must be responsible for superactivation of maximum sliding speed and myosin MgATPase activity.

CONCLUSIONS

The C-terminal mobile domain (Md) of TnI is a critical component for inhibition of striated muscle contraction at resting (diastolic) Ca^{2+} levels, but it is not the sole part of TnI that has this function. Md is not required for superactivation of actomyosin cycling by troponin. Normal Ca^{2+}-regulation of unloaded filament sliding requires tight mechanical coupling between Md and the rest of Tn and Tm.

Acknowledgments

FUNDING

Funding was provided by NIH/NHLBI grant HL63974 to PBC. Funding sources did not have any role in: study design; collection, analysis and interpretation of data; writing or decision to submit this article for publication.

We thank: Linda Stroud for assistance with performing some of the motility assays; Steve Miller in the DNA Sequencing Facility and Rani Dhanarajan in the Molecular Cloning Laboratory of FSU Department of Biological Science's Core Facilities for excellent assistance with generating and validating clones and mutations; and Dr. Brenda Schoffstall for helpful comments on the project.

References

1. Gordon AM, Homsher E, Regnier M. Physiol Rev. 2000; 80:853–924. [PubMed: 10747208]
2. Parmacek MS, Solaro RJ. Prog Cardiovasc Dis. 2004; 47:159–76. [PubMed: 15736582]
3. Gomes AV, Potter JD. Ann New York Acad Sci. 2004; 1015:214–224. [PubMed: 15201162]
4. Willott RH, Gomes AV, Chang AN, Parvatiyar MS, Pinto JR, Potter JD. J Mol Cell Cardiol. 2010; 48:882–92. [PubMed: 19914256]
5. Maron BJ, Maron MS. Lancet. 2013; 381:242–55. [PubMed: 22874472]
6. Sung SS, Brassington AM, Grannatt K, Rutherford A, Whitby FG, Krakowiak PA, Jorde LB, Carey JC, Bamshad M. Am J Hum Genet. 2003; 72:681–90. [PubMed: 12592607]
7. Clarke NF. Adv Exp Med Biol. 2008; 642:40–54. [PubMed: 19181092]
8. Ochala J. J Mol Med. 2008; 86:1197–204. [PubMed: 18574571]
9. Greaser ML, Gergely J. J Biol Chem. 1973; 248:2125–33. [PubMed: 4266138]
10. Syska H, Wilkinson JM, Grand RJ, Perry SV. Biochem J. 1976; 153:375–87. [PubMed: 179535]
11. Van Eyk JE, Hodges RS. J Biol Chem. 1988; 263:1726–1732. [PubMed: 3338991]
12. Van Eyk JE, Thomas LT, Tripet B, Wiesner RJ, Pearlstone JR, Farah CS, Reinach FC, Hodges RS. J Biol Chem. 1997; 272:10529–37. [PubMed: 9099697]
13. Rarick HM, Tu XH, Solaro RJ, Martin AF. J Biol Chem. 1997; 272:26887–92. [PubMed: 9341121]
14. Rarick HM, Tang H-p, Guo X-d, Martin AF, Solaro RJ. J Mol Cell Cardiol. 1999; 31:363–75. [PubMed: 10093049]
15. Vassylyev DG, Takeda S, Wakatsuki S, Maeda K, Maéda Y. Proc Natl Acad Sci USA. 1998; 95:4847–52. [PubMed: 9560191]
16. Takeda S, Yamashita A, Maeda K, Maéda Y. Nature. 2003; 424:35–41. [PubMed: 12840750]
17. Vinogradova MV, Stone DB, Malanina GG, Karatzaferi C, Cooke R, Mendelson RA, Fletterick RJ. Proc Natl Acad Sci USA. 2005; 102:5038–43. [PubMed: 15784741]
18. McKay RT, Pearlstone JR, Corson DC, Gagné SM, Smillie LB, Sykes BD. Biochemistry. 1998; 37:12419–30. [PubMed: 9730814]
19. Li MX, Spyracopoulos L, Sykes BD. Biochemistry. 1999; 38:8289–98. [PubMed: 10387074]
20. Lehman W, Galińska-Rakoczy A, Hatch V, Tobacman LS, Craig R. J Mol Biol. 2009; 388:673–81. [PubMed: 19341744]
21. Galińska-Rakoczy A, Engel P, Xu C, Jung H, Craig R, Tobacman LS, Lehman W. J Mol Biol. 2008; 379:929–35. [PubMed: 18514658]

22. Murakami K, Yumoto F, Ohki S-y, Yasunaga T, Tanokura M, Wakabayashi T. J Mol Biol. 2005; 352:178–201. [PubMed: 16061251]
23. Blumenschein TMA, Stone DB, Fletterick RJ, Mendelson RA, Sykes BD. Biophys J. 2006; 90:2436–44. [PubMed: 16415057]
24. Julien O, Mercier P, Allen CN, Fisette O, Ramos CHI, Lagüe P, Blumenschein TMA, Sykes BD. Proteins. 2011; 79:1240–50. [PubMed: 21322033]
25. Zhang Z, Akhter S, Mottl S, Jin JP. FEBS J. 2011; 278:3348–59. [PubMed: 21777381]
26. Jin JP, Yang FW, Yu ZB, Ruse CI, Bond M, Chen A. Biochemistry. 2001; 40:2623–31. [PubMed: 11327886]
27. Galińska A, Hatch V, Craig R, Murphy AM, Van Eyk JE, Wang CLA, Lehman W, Foster DB. Circ Res. 2010; 106:705–11. [PubMed: 20035081]
28. Zhou Z, Li KL, Rieck D, Ouyang Y, Chandra M, Dong WJ. J Biol Chem. 2012; 287:7661–74. [PubMed: 22207765]
29. Brunet NM, Chase PB, Mihajlović G, Schoffstall B. Arch Biochem Biophys. 2014; 552–553:11–20.
30. Brunet NM, Mihajlović G, Aledealat K, Wang F, Xiong P, von Molnár S, Chase PB. J Biomed Biotechnol. 2012; 2012:657523. [PubMed: 22500102]
31. Wang F, Brunet NM, Grubich JR, Bienkiewicz E, Asbury TM, Compton LA, Mihajlović G, Miller VF, Chase PB. J Biomed Biotechnol. 2011; 2011:435271. [PubMed: 22187526]
32. Schoffstall B, LaBarbera VA, Brunet NM, Gavino BJ, Herring L, Heshmati S, Kraft BH, Inchausti V, Meyer NL, Moonoo D, Takeda AK, Chase PB. DNA Cell Biol. 2011; 30:653–659. [PubMed: 21438758]
33. Schoffstall B, Brunet NM, Wang F, Williams S, Barnes AT, Miller VF, Compton LA, McFadden LA, Taylor DW, Dhanarajan R, Seavy M, Chase PB. J Physiol. 2006; 577:935–944. [PubMed: 17008370]
34. Köhler J, Chen Y, Brenner B, Gordon AM, Kraft T, Martyn DA, Regnier M, Rivera AJ, Wang CK, Chase PB. Physiol Genomics. 2003; 14:117–128. [PubMed: 12759477]
35. Liang B, Chen Y, Wang CK, Luo Z, Regnier M, Gordon AM, Chase PB. Biophys J. 2003; 85:1775–1786. [PubMed: 12944292]
36. Mariano AC, Alexandre GMC, Silva LC, Romeiro A, Cameron LC, Chen Y, Chase PB, Sorenson M. Biochem J. 2001; 358:627–636. [PubMed: 11535124]
37. Chase PB, Chen Y, Kulin K, Daniel TL. Am J Physiol Cell Physiol. 2000; 278:C1088–C1098. [PubMed: 10837336]
38. Gordon AM, Chen Y, Liang B, LaMadrid M, Luo Z, Chase PB. Adv Exp Med Biol. 1998; 453:187–197. [PubMed: 9889829]
39. Gordon AM, LaMadrid M, Chen Y, Luo Z, Chase PB. Biophys J. 1997; 72:1295–1307. [PubMed: 9138575]
40. Regnier M, Martyn DA, Chase PB. Biophys J. 1996; 71:2786–2794. [PubMed: 8913615]
41. Kron SJ, Toyoshima YY, Uyeda TQP, Spudich JA. Methods Enzymol. 1991; 196:399–416. [PubMed: 2034132]
42. Pardee JD, Spudich JA. Methods Enzymol. 1982; 85:164–181. [PubMed: 7121269]
43. Cheng Y, Chen KS, Meyer NL, Yuan J, Hirst LS, Chase PB, Xiong P. Biosens Bioelectron. 2011; 26:4538–4544. [PubMed: 21652197]
44. Gill SC, von Hippel PH. Anal Biochem. 1989; 182:319–26. [PubMed: 2610349]
45. Golitsina N, An Y, Greenfield NJ, Thierfelder L, Iizuka K, Seidman JG, Seidman CE, Lehrer SS, Hitchcock-DeGregori SE. Biochemistry. 1999; 38:3850. [PubMed: 10090775]
46. Monteiro PB, Lataro RC, Ferro JA, Reinach FdC. J Biol Chem. 1994; 269:10461–6. [PubMed: 8144630]
47. Schoffstall B, Clark A, Chase PB. Biophys J. 2006; 91:2216–2226. [PubMed: 16798797]
48. Schoffstall B, Kataoka A, Clark A, Chase PB. J Pharmacol Exp Ther. 2005; 312:12–18. [PubMed: 15306636]
49. Regnier M, Rivera AJ, Chen Y, Chase PB. Circ Res. 2000; 86:1211–1217. [PubMed: 10864910]

50. Butcher MT, Chase PB, Hermanson JW, Clark AN, Brunet NM, Bertram JEA. Am J Physiol Regul Integr Comp Physiol. 2010; 299:R996–R1005. [PubMed: 20702801]
51. Sellers JR, Cuda G, Wang F, Homsher E. Methods Cell Biol. 1993; 39:23–49. [PubMed: 8246800]
52. Sternberg SR. Computer. 1983; 16:22–34.
53. Homsher E, Kim B, Bobkova A, Tobacman LS. Biophys J. 1996; 70:1881–1892. [PubMed: 8785348]
54. Homsher E, Wang F, Sellers JR. Am J Physiol. 1992; 262:C714–C723. [PubMed: 1550212]
55. Hill AV. J Physiol. 1910; 40:iv–vii.
56. Gilda JE, Xu Q, Martinez ME, Nguyen ST, Chase PB, Gomes AV. Arch Biochem Biophys. 2016; doi: 10.1016/j.abb.2016.02.023
57. Sykes BD. Nat Struct Biol. 2003; 10:588–9. [PubMed: 12886291]
58. Kowlessur D, Tobacman LS. J Biol Chem. 2010; 285:38978–86. [PubMed: 20889975]
59. Kowlessur D, Tobacman LS. J Biol Chem. 2010; 285:2686–94. [PubMed: 19920153]
60. Bou-Assaf GM, Chamoun JE, Emmett MR, Fajer PG, Marshall AG. Int J Mass Spectrom. 2011; 302:116–124. [PubMed: 21765647]
61. Martyn DA, Smith L, Kreutziger KL, Xu S, Yu LC, Regnier M. Biophys J. 2007; 92:4379–90. [PubMed: 17400698]
62. Martyn DA, Freitag CJ, Chase PB, Gordon AM. Biophys J. 1999; 76:1480–1493. [PubMed: 10049329]
63. Li KL, Rieck D, Solaro RJ, Dong W. Biophys J. 2014; 107:682–93. [PubMed: 25099807]
64. Kozaili JM, Leek D, Tobacman LS. J Biol Chem. 2010; 285:38034–41. [PubMed: 20889978]
65. James J, Zhang Y, Osinska H, Sanbe A, Klevitsky R, Hewett TE, Robbins J. Circ Res. 2000; 87:805–11. [PubMed: 11055985]
66. Elliott K, Watkins H, Redwood CS. J Biol Chem. 2000; 275:22069–74. [PubMed: 10806205]
67. Takahashi-Yanaga F, Morimoto S, Harada K, Minakami R, Shiraishi F, Ohta M, Lu QW, Sasaguri T, Ohtsuki I. J Mol Cell Cardiol. 2001; 33:2095–107. [PubMed: 11735257]
68. Tardiff JC. Circ Res. 2011; 108:765–82. [PubMed: 21415410]
69. Tardiff JC. Heart Fail Rev. 2005; 10:237–48. [PubMed: 16416046]
70. Gomes AV, Liang J, Potter JD. J Biol Chem. 2005; 280:30909–15. [PubMed: 15961398]
71. Gomes AV, Potter JD. Mol Cell Biochem. 2004; 263:99–114. [PubMed: 15524171]
72. Akhter S, Bueltmann K Jr, Huang X, Jin J-P. Arch Biochem Biophys. 2014; 552–553:3–10.
73. Davis J, Wen H, Edwards T, Metzger JM. Circ Res. 2007; 100:1494–502. [PubMed: 17463320]
74. Li Y, Zhang L, Jean-Charles PY, Nan C, Chen G, Tian J, Jin JP, Gelb IJ, Huang X. J Mol Cell Cardiol. 2013; 62:227–36. [PubMed: 23810866]
75. Yumoto F, Lu QW, Morimoto S, Tanaka H, Kono N, Nagata K, Ojima T, Takahashi-Yanaga F, Miwa Y, Sasaguri T, Nishita K, Tanokura M, Ohtsuki I. Biochem Biophys Res Commun. 2005; 338:1519–1526. [PubMed: 16288990]
76. Shrimpton AE, Hoo JJ. Eur J Med Genet. 2006; 49:201–6. [PubMed: 16497570]
77. Jiang M, Zhao X, Han W, Bian C, Li X, Wang G, Ao Y, Li Y, Yi D, Zhe Y, Lo WH, Zhang X, Li J. Hum Genet. 2006; 120:238–42. [PubMed: 16802141]
78. Kimber E, Tajsharghi H, Kroksmark AK, Oldfors A, Tulinius M. Neurology. 2006; 67:597–601. [PubMed: 16924011]
79. McDonough JL, Arrell DK, Van Eyk JE. Circ Res. 1999; 84:9–20. [PubMed: 9915770]
80. Murphy AM, Kögler H, Georgakopoulos D, McDonough JL, Kass DA, Van Eyk JE, Marbán E. Science. 2000; 287:488–91. [PubMed: 10642551]
81. Foster DB, Noguchi T, VanBuren P, Murphy AM, Van Eyk JE. Circ Res. 2003; 93:917–24. [PubMed: 14551240]
82. Narolska NA, Piroddi N, Belus A, Boontje NM, Scellini B, Deppermann S, Zaremba R, Musters RJ, dos Remedios C, Jaquet K, Foster DB, Murphy AM, van Eyk JE, Tesi C, Poggesi C, van der Velden J, Stienen GJM. Circ Res. 2006; 99:1012–20. [PubMed: 17023673]

83. Strauss JD, Zeugner C, Van Eyk JE, Bletz C, Troschka M, Rüegg JC. FEBS Lett. 1992; 310:229–234. [PubMed: 1397278]
84. Homsher E, Nili M, Chen IY, Tobacman LS. Biophys J. 2003; 85:1046–52. [PubMed: 12885651]
85. Homsher E, Lee DM, Morris C, Pavlov D, Tobacman LS. J Physiol. 2000; 524:233–243. [PubMed: 10747195]
86. Clemmens EW, Entezari M, Martyn DA, Regnier M. J Physiol. 2005; 566:737–746. [PubMed: 15905219]
87. Clemmens EW, Regnier M. J Muscle Res Cell Motil. 2004; 25:515–25. [PubMed: 15711882]
88. Fraser IDC, Marston SB. J Biol Chem. 1995; 270:7836–7841. [PubMed: 7713874]
89. Brown JH, Kim K-H, Jun G, Greenfield NJ, Dominguez R, Volkmann N, Hitchcock-DeGregori SE, Cohen C. Proc Natl Acad Sci USA. 2001; 98:8496–501. [PubMed: 11438684]
90. Loong CKP, Zhou HX, Chase PB. PLoS One. 2012; 7:e39676. [PubMed: 22737252]

HIGHLIGHTS

- Cardiac troponin I C-terminal mobile domain was assayed by Ca^{2+}-regulated motility
- In one construct Md was partially decoupled from Tn by a short flexible linker
- In another construct Md was eliminated entirely
- Md primarily stabilizes off state of thin filament regulatory units at low Ca^{2+}
- Confirmed Md is not responsible for superactivation of actomyosin cycling by Tn

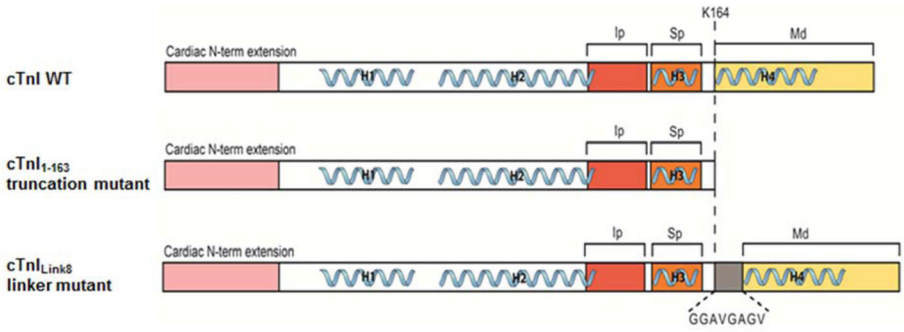

FIGURE 1.

WT and two modified cTnI constructs ($cTnI_{1\text{-}163}$ and $cTnI_{Link8}$) generated for this study. Residues 1–163 are common to all three proteins, and include the cardiac-specific N-terminal extension, inhibitory peptide (Ip), and switch peptide (Sp). Construct $cTnI_{1\text{-}163}$ is missing the entire C-terminal mobile domain (Md) that is present in WT and $cTnI_{Link8}$. Construct $cTnI_{Link8}$ has a short, 8-amino acid, flexible linker inserted before Md, as indicated below the schematic (see Materials and methods). Locations of structural α-helices 1–4 (H1–H4) are indicated.

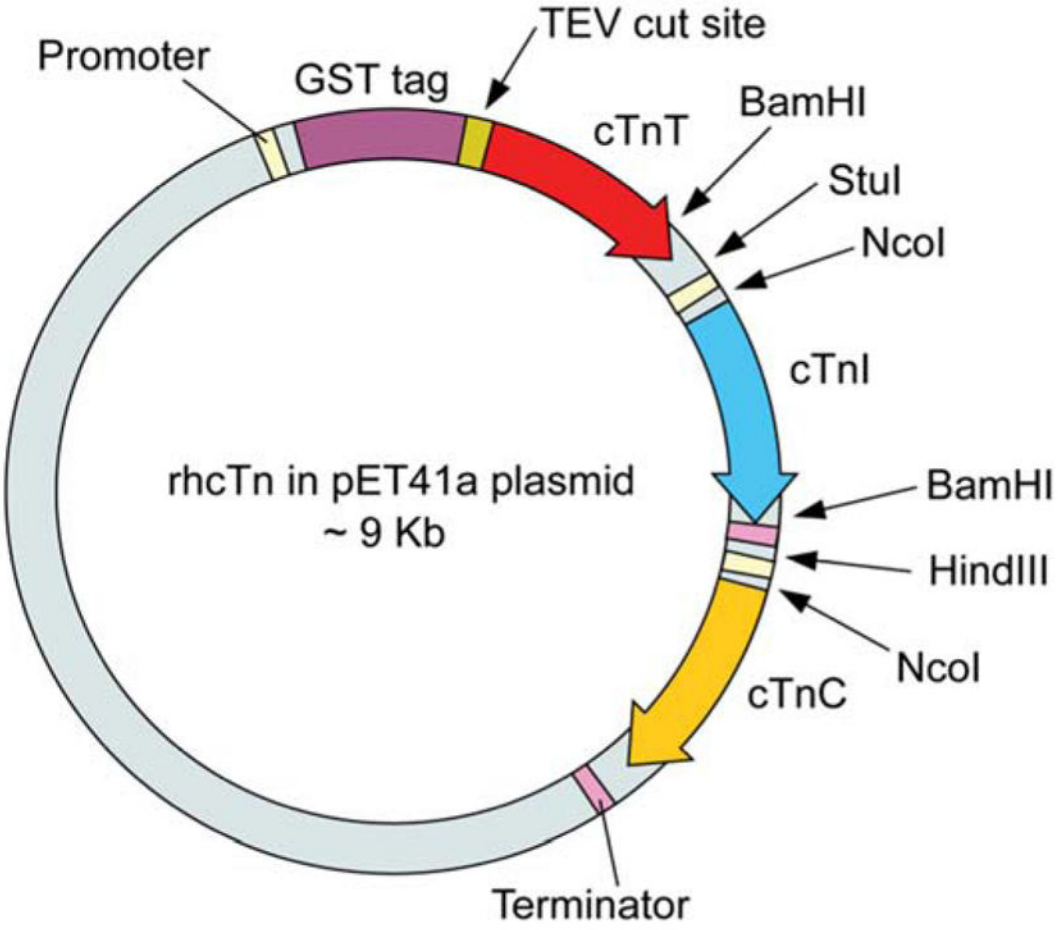

FIGURE 2.

Schematic of modified pET41a rhcTn co-expression vector showing placement of gene sequences for the three troponin subunits, the GST affinity tag at cTnT's N-terminus for purification of ternary troponin complex, and the site for TEV proteolytic removal of the GST affinity tag. The three troponin subunits are translated as separate polypeptides. Altered cTnI constructs $cTnI_{1\text{-}163}$ or $cTnI_{Link8}$ (Fig. 1) replaced "cTnI" sequence for bacterial co-expression of modified troponins as described in Materials and methods.

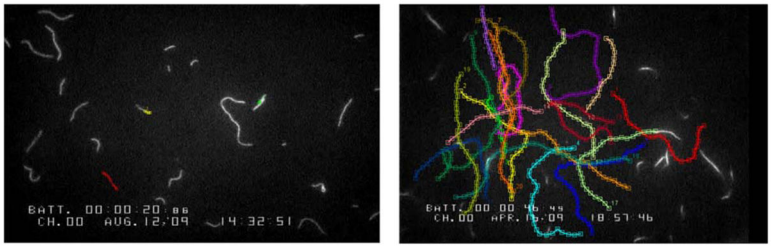

FIGURE 3.

Analysis of filament sliding in motility assays. Representative examples of regulated WT filaments tracked at pCa 9 (left) or pCa 5 (right). Each color indicates a distinct filament trajectory determined from sequential images in the time series (for details see Materials and methods). Filaments not marked with a color trajectory (pCa 9) displayed no discernible translocation. Average speed (in μm/s) was obtained by dividing the distance traveled (in μm) by the duration of tracking (in s).

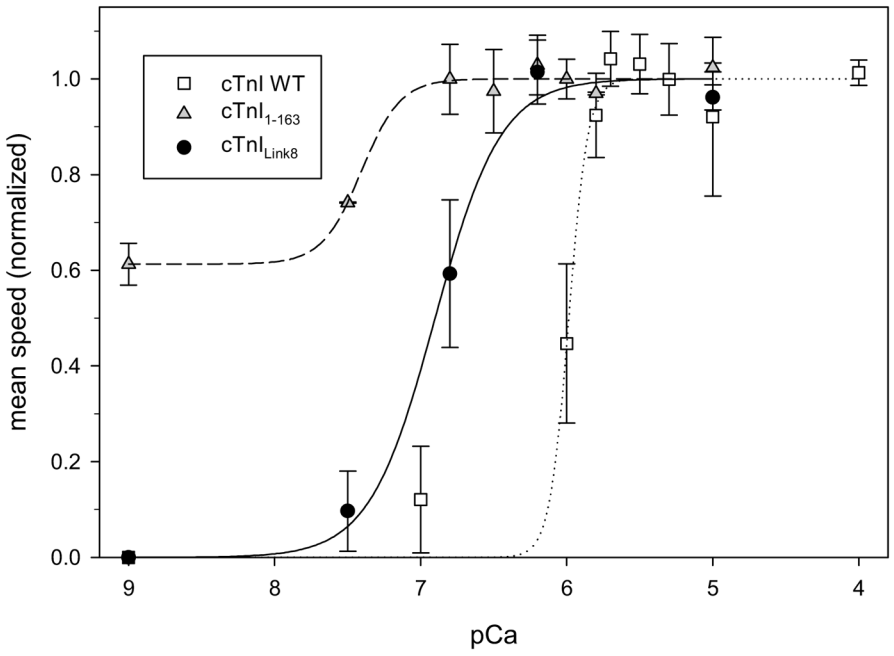

FIGURE 4.

Ca^{2+}-dependence of sliding speed of reconstituted thin filaments with rhcTn containing either cTnI WT (open squares and dotted line), $cTnI_{Link8}$ (solid circles and solid line), or $cTnI_{1\text{-}163}$ (gray triangles and dashed line). Points are normalized mean speed (*s*) + SD. Lines are nonlinear least squares regression fits to Eq 2 (WT and $cTnI_{Link8}$) or Eq 3 ($cTnI_{1\text{-}163}$). Regression parameter estimates are given in Table 1.

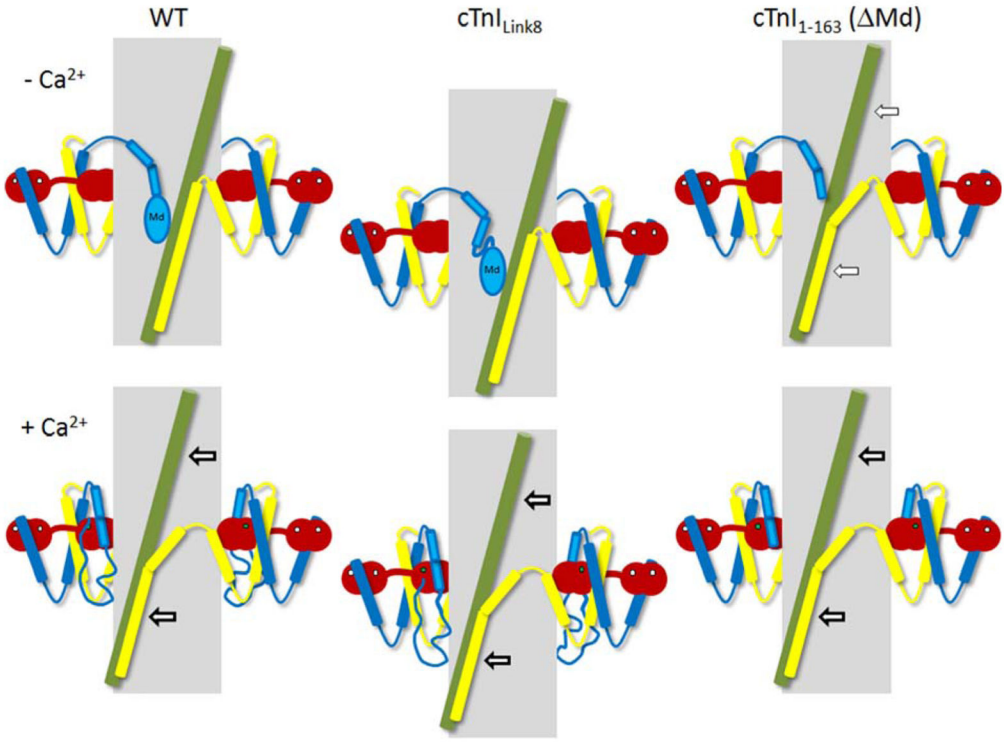

FIGURE 5.

Schematic representation of the three cTnI constructs (WT, left; cTnI$_{Link8}$, middle; and cTnI$_{1-163}$, right) in the context of part of thin filament regulatory units in the absence (top) or presence (bottom) of activating Ca^{2+}. Actin is gray and Tm is green; activation of a regulatory unit is indicated by leftward displacement of Tm on actin (arrows). cTnT is yellow; the α-helical N-terminus of cTnT is associated with Tm at the bottom of each panel. cTnC is red. In the absence of Ca^{2+} (top panels), up to two Mg^{2+} ions (white dots) bind to the EF-hand sites III and IV in the C-domain of cTnC. In the presence of activating Ca^{2+} (bottom panels), up to one Ca^{2+} ion (green dot) binds to site II in the N-domain of cTnC, while up to two divalent cations (Mg^{2+} or Ca^{2+}; white dots) bind to the C-domain of cTnC. cTnI is blue. The coiled-coil IT-arm is schematically illustrated as a cross-over between portions of cTnI and cTnT. Following cTnI from the IT-arm, the C-terminus of cTnI is shown with emphasis, sequentially, on the inhibitory peptide (first light blue segment), switch peptide (second light blue segment), the eight amino acid linker (heavy blue line) in cTnI$_{Link8}$ (middle panel), and in WT (left) and cTnI$_{Link8}$ (middle), the mobile domain (Md, labeled light blue oval in the top left and middle panels only); note that the presumed unfolding of Md in the presence of Ca^{2+} [23,24] is illustrated for WT (bottom left) and cTnI$_{Link8}$ (bottom middle). In each of the six scenarios, two troponin molecules are shown, representing complexes associated with the two strands of Tm that wrap around each thin filament (only one Tm is visible in this orientation). Note that the relative scaling is approximate, and that the activation-related displacements of Ip and Sp are exaggerated for clarity. Activation of a regulatory unit involves cooperative interactions of the two troponins, with particularly important roles for the C-terminal regions of both molecules of cTnI, along the lines previously envisioned [20,21]. Missing from this schematic representation is the

cardiac-specific N-terminus of cTnI. Also missing from these static images are protein dynamics: dynamics of regulatory units involving Ca^{2+} binding and dissociation (particularly at intermediate Ca^{2+} levels); and dynamic motions within and between proteins. In addition, the structural kinks and flexibility of Tm are also missing [89,90].

TABLE 1

Regression results from fits of Eq 2 (WT and $cTnI_{Link8}$) or Eq 3 ($cTnI_{1-163}$) to normalized motility speed-pCa data shown in Fig. 4.

Parameter	WT	$cTnI_{Link8}$	$cTnI_{1-163}$
R^2	0.982	0.993	0.982
n_H	6.6 ± 2.4	1.9 ± 0.4	3.2 ± 3.6
pCa_{50}	5.99 ± 0.02	6.90 ± 0.04	7.41 ± 0.11
s_{min}	0	0	0.61 ± 0.02
s_{max}	1	1	0.39

Nonlinear least squares regressions were performed on normalized speed data (s) as described in Materials and methods. Errors for regression parameter estimates are SE for the regression. Note that, by definition for Eq 2 (WT and $cTnI_{Link8}$), $s_{min} = 0$ and $s_{max} = 1$. Also note that, by definition for Eq 3 ($cTnI_{1-163}$), $s_{max} = 1 - s_{min}$.